Available online at www.sciencedirect.com
SCIENCE DIRECT®
Journal of the European Ceramic Society 26 (2006) 247–251
www.elsevier.com/locate/jeurceramsoc

# New double-ceramic-layer thermal barrier coatings based on zirconia–rare earth composite oxides

X.Q. Cao[a,*], R. Vassen[b], F. Tietz[b], D. Stoever[b]

[a] *Key Laboratory of Rare Earth Chemistry and Physics, Changchun Institute of Applied Chemistry, Chinese Academy of Sciences, Changchun, 130022 Jilin, China*
[b] *Institut für Werkstoffe der Energietechnik (IWV-1), Forschungszentrum Juelich GmbH, 52425 Juelich, Deutschland*

Received 20 May 2004; received in revised form 12 October 2004; accepted 12 November 2004
Available online 12 January 2005

**Abstract**

A series of $La_2O_3$–$ZrO_2$–$CeO_2$ composite oxides were synthesized by solid-state reaction. The final product keeps fluorite structure when the molar ratio $Ce/Zr \geq 0.7/0.3$, and below this ratio only mixtures of $La_2Zr_2O_7$ (pyrochlore) and $La_2O_3$–$CeO_2$ (fluorite) exist. Averagely speaking, the increase of $CeO_2$ content gives rise to the increase of thermal expansion coefficient and the reduction of thermal conductivity, but $La_2(Zr_{0.7}Ce_{0.3})_2O_7$ has the lowest sintering ability and the lowest thermal conductivity which could be explained by the theory of phonon scattering. Based on the large thermal expansion coefficient of $La_2Ce_{3.25}O_{9.5}$, the low thermal conductivities and low sintering abilities of $La_2Zr_2O_7$ and $La_2(Zr_{0.7}Ce_{0.3})_2O_7$, double-ceramic-layer thermal barrier coatings were prepared. The thermal cycling tests indicate that such a design can largely improve the thermal cycling lives of the coatings. Since no single material that has been studied so far satisfies all the requirements for high temperature thermal barrier coatings, double-ceramic-layer coating may be an important development direction of thermal barrier coatings.


*Keywords:* Thermal properties; $CeO_2$; $ZrO_2$; Structural applications; Thermal barrier coatings

## 1. Introduction

During the last decade, research efforts were devoted to the development and manufacturing of ceramic thermal barrier coatings (TBCs) on turbine parts because the traditional turbine materials have reached the limits of their temperature capabilities. TBCs are deposited on transition pieces, combustion lines, first-stage blades and vanes and other hot-path components of gas turbines either to increase the inlet temperature with a consequent improvement of the efficiency or to reduce the requirements for the cooling system.[1–3] Besides the 8YSZ (8 wt.% $Y_2O_3$ + 92 wt.% $ZrO_2$) nowadays as the standard TBC material, several other ceramic materials such as zirconia stabilized with calcium oxide or magnesium oxide, mullite, composites of $CeO_2$ and 8YSZ, zircon and $La_2Zr_2O_7$ (LZ), etc. have been evaluated as TBC materials.[4]

The selection of TBC materials is restricted by some basic requirements such as high melting point, no phase transformation between room temperature and operation temperature, low thermal conductivity, chemical inertness, thermal expansion match with the metallic substrate, good adherence to the metallic substrate and low sintering rate of the porous microstructure.[1,5] The number of materials that can be used as TBCs is very limited. Because no single material satisfies all requirements for TBCs, it seems that the concept of multilayer is effective for the improvement of the thermal shock life of TBCs.[6,7] The multilayer includes an erosion resistant layer as the outer layer, a thermal barrier layer, a corrosion–oxidation resistant layer, a thermal stress control layer and a diffusion resistant layer. Based on the multilayer system, a double-ceramic-layer (DCL) coating of 8YSZ and LZ is newly developed.[8] On top of the 8YSZ layer, a LZ layer

* Corresponding author.
*E-mail address:* xcao@ciac.jl.cn (X.Q. Cao).

0955-2219/$ – see front matter © 2004 Elsevier Ltd. All rights reserved.
doi:10.1016/j.jeurceramsoc.2004.11.007

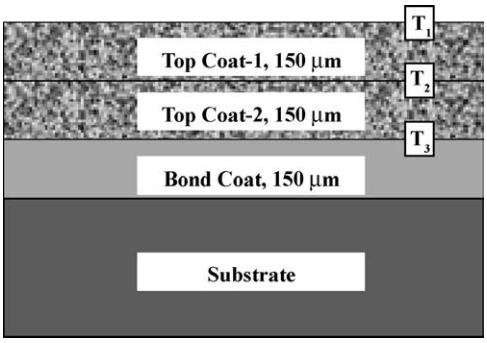


Fig. 1. Theory of DCL coating.

is formed. In the DCL coating, the top ceramic layer should have a low thermal conductivity and high phase stability, and it acts as a thermal insulator to protect the inner layer. As reported by the authors, the thermal cycling performance of 8YSZ/LZ (LZ on top of 8YSZ) coating is excellent, and the 8YSZ/$CeO_2$ ($CeO_2$ on top of 8YSZ) coating showed a good thermal shock resistance.[9] In this work, other DCL coatings of composite oxides $La_2O_3$–$ZrO_2$–$CeO_2$ were studied, and in Fig. 1 is shown the design of such a DCL coating.

## 2. Experimental

Main chemicals used in this work were $La_2O_3$ (99.9%, Aldrich), $ZrO_2$ (99%, Aldrich), $CeO_2$ (99.9%, Aldrich). The starting powder for plasma-sprayed coatings was synthesized by firing a mixture of corresponding oxides and spray-drying (particle size 45–80 μm). Crystal structure was analyzed by X-ray Diffraction (XRD, STADI Diffractometer, Co Kα radiation). Thermal expansion and sintering ability of the materials were recorded with a high temperature dilatometer (Netzsch 402 E). Samples for dilatometric and thermal conductivity measurements were prepared by cold-pressing and then sintering at 1923 K for 6 h with heating and cooling rates of 180 K/h. Sintered samples were cut into small bars with length 25 mm or small pellets with diameter 9.0 mm and height 2.0 mm for dilatometric or thermal diffusivity measurement, respectively. Thermal diffusivity measurements were made by using a laser flash apparatus (Port Washington THETA). Heat capacity measurements were performed between room temperature and 1573 K using a thermal analyzer (Netzsch STA 429). Plasma-sprayed coatings were produced by atmospheric spraying with a Sulzer Metco Triplex Gun, and parameters are: plasma gas Ar/He = 12/23 standard litter per minute, current = 299 A, voltage = 69 V, coating distance = 80 mm. The coatings for thermal cycling were made by spraying on a superalloy substrate (IN738) with a NiCoCrAlY bond coat (thickness ∼150 μm). The thermal cycling tests were carried out with a methane/oxygen flame, and the coating surface (diameter 3 cm) was cycled from room temperature to 1523 K within 20 s. The total heating time was 5 min, followed by quenching to room temperature within 2 min by a cooling air jet. The substrate temperature was about 1243 K. Once a large crack in the coating was formed, the temperature of the substrate would be increased immediately and the test would be stopped automatically, and the given cycling number corresponds to the thermal cycling life of the coating. Symbols for the samples are listed in Table 1.

## 3. Results and discussion

The XRD patterns of $La_2(Zr_{1-x}Ce_x)_2O_7$ are shown in XRD Fig. 2. The peaks of $La_2Ce_2O_7$ (LC, fluorite) shift to the large 2$\theta$-side (lattice parameter decreased) and those of LZ (pyrochlore) to the small 2$\theta$-side (lattice parameter increased), indicating that $Ce^{4+}$ and $Zr^{4+}$ are replaced by each other. Furthermore, it is clear that the solubility of $La_2Zr_2O_7$ in $La_2Ce_2O_7$ is close to 70% (i.e. composition $La_2(Zr_{0.3}Ce_{0.7})_2O_7$) but the solubility of $La_2Ce_2O_7$ in $La_2Zr_2O_7$ is lower than 10%. Similar phenomenon was observed for the $Nd_2Ce_2O_7$–$Nd_2Zr_2O_7$ system by Dixon et al.[10] $Nd_2Zr_2O_7$ (pyrochlore) can solute in $Nd_2Ce_2O_7$ (fluorite) for about 50%, but for only 5–10% can $Nd_2Ce_2O_7$ solute in $Nd_2Zr_2O_7$, between 10 and 50% mixtures of pyrochlore and fluorite were formed.

For the dilatometric measurement, the coating was heated from room temperature upto 1673 K with a heating rate of 180 K/h and then held for 15 h. Both the temperature profile and the dilatometric curve of the plasma-sprayed coating

Table 1
Compositions of the powders and their plasma-sprayed coatings

| Starting powder composition | Coating composition | Symbol for the coating | $\alpha$[a] of the coating ($\times 10^{-6}$ K$^{-1}$) | $T_{sintering}$[b] of the coating (K) |
|---|---|---|---|---|
| $La_2Ce_2O_7$ | $La_2Ce_{1.229}O_{5.458}$ | LC | 10.91 (453–1473 K) | 1518 |
| $La_2Ce_{3.25}O_{9.5}$ | $La_2Ce_{2.358}O_{7.717}$ | LC3.25 | 12.84 (453–1473 K) | 1613 |
| $La_2(Zr_{0.3}Ce_{0.7})_2O_7$ | $La_2(Zr_{0.386}Ce_{0.441})_2O_{6.307}$ | LZ3C7 | 9.36 (593–1473 K) | 1578 |
| $La_2(Zr_{0.7}Ce_{0.3})_2O_7$ | $La_2(Zr_{0.663}Ce_{0.268})_2O_{6.724}$ | LZ7C3 | 8.90 (453–1473 K) | 1663 |
| $La_2(Zr_{0.773}Ce_{0.331})_2O_{7.419}$ | $La_2(Zr_{0.745}Ce_{0.386})_2O_{7.524}$ | LZ7C3-mix[c] | 10.71 (453–1473 K) | No sintering |
| $La_2Zr_2O_7$ | $La_{1.72}Zr_2O_{6.58}$ | LZ | 10.91 (453–1473 K) | 1663 |

[a] $\alpha$, thermal expansion coefficient.
[b] $T_{sintering}$, sintering temperature.
[c] LZ7C3-mix, the coating whose starting powder is a mixture of 30 mol% LC3.25 and 70 mol% LZ.

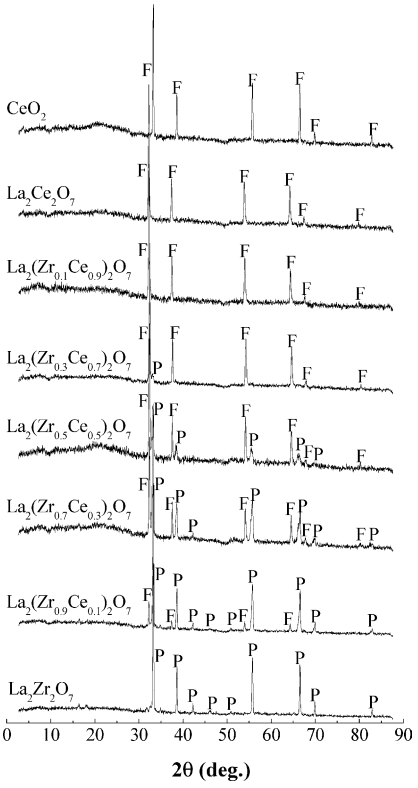


Fig. 2. XRD patterns of $La_2(Zr_{1-x}Ce_x)_2O_7$, Co Kα radiation. Symbols P and F for pyrochlore and fluorite-type structures, respectively.

are shown in Fig. 3. In the dilatometric curve, the maximum temperature at which the coating begins to contract instead of expansion is named as "sintering temperature, $T_{sintering}$". The sintering temperatures of these coatings are listed in Table 1. The coating LC has a higher sintering ability than LZ and normally the sintering ability increases with the increase of

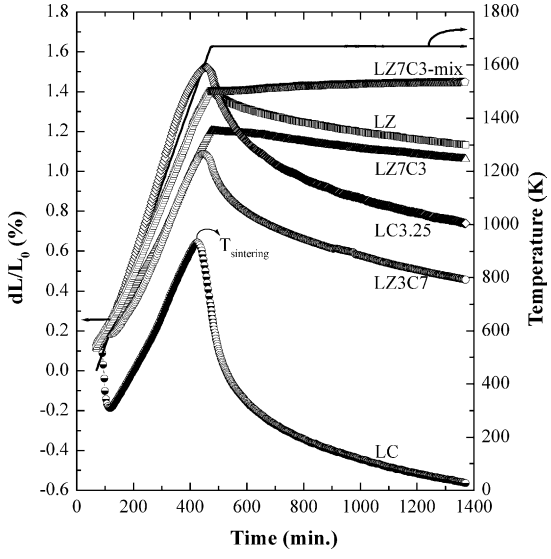


Fig. 3. Dilatometric measurements of $La_2(Zr_{1-x}Ce_x)_2O_7$ plasma-sprayed coatings.

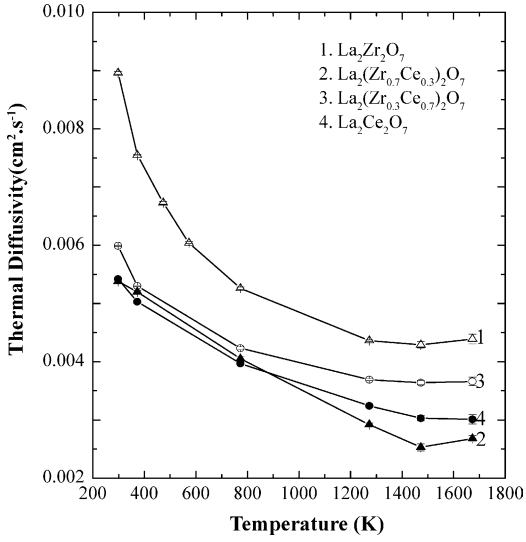


Fig. 4. Thermal diffusivities of $La_2(Zr_{1-x}Ce_x)_2O_7$ as functions of temperature.

$CeO_2$ content. However, it is very interesting to find that the coating in which the Zr/Ce ratio is 0.7/0.3 has the lowest sintering ability and even the coating LZ7C3-mix slightly expands instead of shrinking. On the other hand, the sample in which the Zr/Ce ratio is 0.7/0.3 has the lowest thermal diffusivity (Fig. 4). The thermal diffusivity decreases with the increase of temperature till about 1450 K followed by a slight increase. The thermal conduction can be explained by the theory of phonon scattering. In ceramics, heat transport via phonons (lattice vibrations) are the major mechanism of thermal conductivity.[11] For $La_2(Zr_{1-x}Ce_x)_2O_7$, this mechanism seems to be dominant below 1450 K and above this temperature the radiation effect becomes more significant. The composite material usually has a lower thermal conductivity than those of pure materials due to the reduction of free path length of the phonons. According to this mechanism, in ceramics made of solid solutions or composites, the regularity of the crystal structure is altered and the phonons are more scattered resulting in a decrease of conductivity. As shown in Fig. 2, LZ3C7 is nearly a pure material with fluorite structure and its thermal conductivity is lower than that of LZ and higher than that of LC, but LZ7C3 is a composite of LZ and LC and therefore it is not curious that it has the lowest thermal conductivity. Composites of $CeO_2$ with 5–20 wt.%

Table 2
Thermal cycling lives of DCL coatings

| Coating | Life (cycles to failure) |
|---|---|
| LC3.25 (339 μm) | 29 |
| LZ7C3-mix (305 μm) | 120 |
| LC3.25 (105 μm)/LZ7C3-mix (185 μm) | 225 |
| LC3.25 (113 μm)/LZ (181 μm) | 150 |
| LZ | 35 |

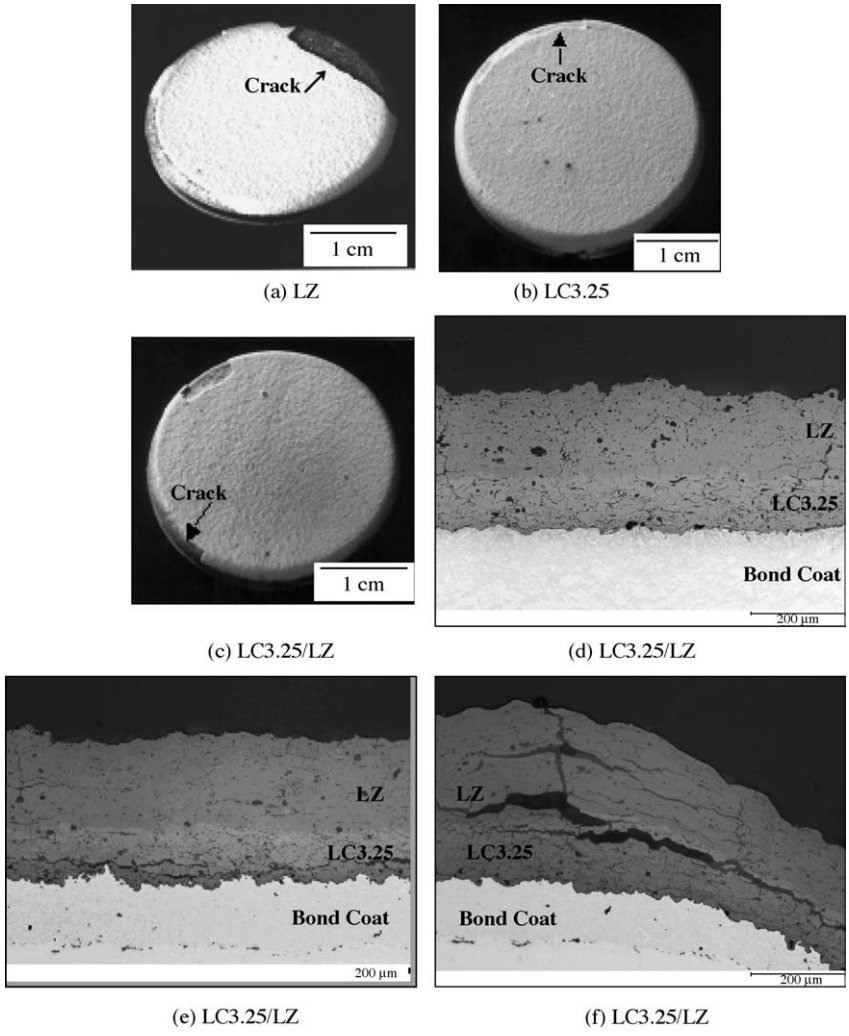


Fig. 5. Surface photographs and microstructures of coatings after thermal cycling: (a) LZ; (b) LC3.25; (c–f) LC3.25/LZ, central part before thermal cycling (d), central part (e) and rim (f) after thermal cycling.

$Al_2O_3$ also have lower thermal diffusivities than pure $CeO_2$ and $Al_2O_3$ even though pure $Al_2O_3$ has high thermal diffusivity and $CeO_2$ has a low value.[12]

Due to the large thermal expansion coefficient of LC3.25, the low sintering ability and low thermal conductivity of LZ7C3 and LZ, it is a great hope that these materials will exhibit new layered coatings with the LZ7C3 or LZ coating on top of the LC3.25 coating for good thermal protection. The coating design is shown in Fig. 1. The top coating material is either LZ7C3 or LZ. If the thermal cycling condition is $T_1/T_3 = 1523\,K/1243\,K$, then the surface temperature of the LC3.25 layer ($T_2$) should be 1393 K which is about 225 K lower than its sintering temperature (1618 K). The calculation is based on the thermal conductivities of LZ7C3 ($0.52\,W\,m^{-1}\,K^{-1}$, relative density ± 70%, 150 μm) and LC3.25 ($0.6\,W\,m^{-1}\,K^{-1}$, relative density ± 70%, 150 μm). The steady state heat conduction obeys the following equation:

$$j = -\lambda \frac{dT}{dl}$$

where $j$ is the heat flux; λ, thermal conductivity; $T$, temperature and $l$, thickness of the coating.

The coating experiments arrangement and the thermal cycling lives of those coatings are compared in Table 2.

For comparison, the photographs of LZ, LC3.25 and LC3.25/LZ after thermal cycling are shown in Fig. 5. The crack within the LZ coating looks like that the whole coating spalls off the substrate, which can be explained by the small thermal expansion coefficient and low toughness of LZ. Both DCL coatings of LC3.25/LZ and LC3.25/LZ7C3-mix spalled mainly at the interface between the top layer and the bottom layer. As shown in Fig. 5c, the coating LC3.25/LZ failed at the rim where a thin layer of the coating, namely LC3.25, can still be observed on the substrate. The microstructures before and after thermal cycling are compared in Fig. 5d–f. The crack of the coating at the rim seems to be

a result of thermal expansion mismatch between LC3.25 and LZ.

## 4. Conclusion

The thermal cycling lives of LC3.25 coating, LZ7C3-mix coating and LZ coating are short, but their DCL coatings can largely improve their lives, indicating that this is an efficient way to use the advantages and overcome the disadvantages of coating materials. This may be a new development direction of TBCs. For the here tested DCL coatings, the thermal expansion mismatch between the top and bottom coating materials is the main failure mechanism. Between these two layers, if a functionally graded coating is formed, this problem would be hopefully reduced.

## Acknowledgements

The authors thank Mr. W. Reichert (Forschungszentrum Juelich, FZJ, Germany) for XRD measurements, Mr. W. Jungen for spray-drying, Mr. Karl-Heinz Rauwald and Mr. Ralf Laufs (FZJ) for their invaluable assistance during plasma spraying and thermal cycling tests. Main experiments in this paper were carried out in FZJ and the rest work was finished in Changchun Institute of Applied Chemistry and financially supported by “Bai Ren” & “863” Projects (2002AA332010).

## References

1. Cernuschi, F., Bianchi, P., Leoni, M. and Scardi, P., Thermal diffusivity/microstructure relationship in Y-PSZ thermal barrier coatings. *J. Therm. Spray Technol.*, 1999, **8**(1), 102–109.
2. DeMasi-Marcin, J. T. and Gupta, D. K., Protective coatings in the gas turbine engine. *Surf. Coat. Technol.*, 1994, **68/69**, 1–9.
3. Wigren, J. and Pejryd, L., Thermal barrier coatings-why, how, where and where to. In *Proceedings of the 15th International Thermal Spray Conference: Thermal Spray Meeting the Challenges of the 21st Century*, ed. C. Coddet. ASM International, Materials Park, OH, USA, 1998, pp. 1531–1542.
4. Cao, X. Q., Vassen, R. and Stoever, D., Ceramic materials for thermal barrier coatings. *J. Eur. Ceram. Soc.*, 2004, **24**, 1–10.
5. Vassen, R., Tietz, F., Kerkhof, G. and Stoever, D., New materials for advanced thermal barrier coatings. In *Proceedings of the 6th Liege Conference on Materials for Advanced Power Engineering*, ed. J. Lecomte-Beckers, F. Schubert and P. J. Ennis. Forschungszentrum Juelich GmbH, Juelich, Deutschland, 1998, pp. 1627–1635.
6. Tamura, M., Takahashi, M., Ishii, J., Suzuki, K., Sato, M. and Shimomura, K., Multilayered thermal barrier coating for land-based gas turbines. *J. Therm. Spray Technol.*, 1999, **8**(1), 68–72.
7. Takahashi, M., Itoh, Y. and Miyazaki, M., Thermal barrier coatings design for gas turbine. In *Proceedings of 14th International Thermal Spraying (Vol 1)*, ed. A. Ohmori. High Temperature Society of Japan, Kobe, Japan, 1995, pp. 83–88.
8. Vassen, R., Dietrich, M., Lehmann, H., Cao, X., Pracht, G., Tietz, F. *et al.*, Development of oxide ceramics for an application as TBC. *Mater. Sci. Eng. Technol.*, 2001, **32**(8), 673–677.
9. Wilden, J. and Wank, A., Application study on ceria based thermal barrier coatings. *Mater. Sci. Eng. Technol.*, 2001, **32**(8), 654–659.
10. Dixon, S., Marr, J., Lachowski, E. E., Gard, J. A. and Glasser, F. P., Preparation and properties of some phases in the system $Nd_2O_3$–$CeO_2$–$ZrO_2$–$RuO_2$. *Mater. Res. Bull.*, 1980, **15**(12), 1811–1816.
11. Van Vlack, L. H., Thermal properties and high-temperature behaviour. In *Physical Ceramics for Engineering*. Addison-Wesley, 1964, p.140.
12. Vassen, R., Cao, X., Tietz, F., Basu, D. and Stoever, D., Zirconates as new materials for thermal barrier coatings. *J. Am. Ceram. Soc.*, 2000, **83**(8), 2023–2028.